

ORIGINAL ARTICLE

Combination effects of ellagic acid with erlotinib in a Ba/F3 cell line expressing *EGFR* H773_V774 insH mutation

Chuanqi Xie^{1,2} , Jindong Kong^{1,2}, Fujun Miao^{1,2}, Xuanjun Wang^{1,3,4} & Jun Sheng^{1,4}

1 Key Laboratory of Pu-er Tea Science, Ministry of Education, Yunnan Agricultural University, Kunming, China

2 College of Food Science and Technology, Yunnan Agricultural University, Kunming, China

3 College of Science, Yunnan Agricultural University, Kunming, China

4 State Key Laboratory for Conservation and Utilization of Bio-Resources in Yunnan, Kunming, China

Keywords

EGFR H773_V774 insH mutation; Ba/F3 cell line; ellagic acid; erlotinib; combination effects.

Correspondence

Xuanjun Wang, College of Science, Yunnan Agricultural University, Fengyuan Road 452th, Kunming, 650201, China.

Tel: +86 15912579655

Fax: (0871)65221788

Email: jwang@ynau.edu.cn

Jun Sheng, Yunnan Agricultural University, Fengyuan Road 452th, Kunming, 650201, China.

Tel: +86 13888036266

Fax: (0871)65221788

Email: shengj@ynau.edu.cn

Received: 24 March 2020;

Accepted: 28 April 2020.

doi: 10.1111/1759-7714.13487

Thoracic Cancer **11** (2020) 2101–2111

Abstract

Background: Epidermal growth factor receptor H773_V774 insH (*EGFR*-insH) is an *EGFR* exon 20 insertion mutation in non-small cell lung cancer (NSCLC), which is naturally resistant to available *EGFR* tyrosine kinase inhibitors (TKIs) and lacks a patient-derived cell line.

Methods: A Ba/F3 cell line expressing *EGFR*-insH mutation (Ba/F3-insH cell line) was generated using an IL3-deprivation method. A cell proliferation assay was performed to screen natural compounds that exhibit a synergistic effect with erlotinib. Trypan blue staining was used to assess cell growth and crystal violet staining was recruited to evaluate clonogenic potential. Flow cytometry was used to detect *EGFR* expression and cell apoptosis. A xenograft model was created to evaluate the effect of ellagic acid (EA) with erlotinib on tumor growth.

Results: EA was identified to synergistically inhibit the proliferation of Ba/F3-insH cells with erlotinib. The growth and clonogenic potential of Ba/F3-insH cells were definitely constrained by EA with erlotinib, whereas, the apoptosis of Ba/F3-insH cells was dramatically promoted by the combination. In a xenograft model of the Ba/F3-insH cell line, the combination treatment also exhibited a synergistic reduction in tumor growth.

Conclusions: In this study, we generated a Ba/F3 cell line expressing *EGFR* H773_V774 insH mutation and identified a synergistic treatment (EA with erlotinib) that markedly inhibited the viability of Ba/F3-insH cells in vitro and in vivo.

Key points

Our results indicated that the combination of ellagic acid with erlotinib has synergistic effects against *EGFR* H773_V774 insH mutation.

Introduction

Lung cancer is the most commonly diagnosed cancer and the leading cause of cancer-related death in the world, with non-small cell lung cancer (NSCLC) comprising the vast majority (85%) of all lung carcinomas.^{1–3} Epidermal growth factor receptor (*EGFR*) gene mutations, which account for approximately 10%–15% of NSCLCs, defined a prevalent molecularly-classified subgroup of NSCLC.^{4, 5} The first group of *EGFR* mutations containing in-frame deletions of exon 19 (45% of *EGFR* mutations) and exon

21 L858R point mutation (40% of *EGFR* mutations), has been found to respond to monotherapy with *EGFR* tyrosine kinase inhibitors (TKIs) gefitinib and erlotinib.^{6–11} However, the other main group in NSCLC, composed of in-frame insertions within exon 20 (4%–10% of all *EGFR* mutations), is intrinsically resistant to *EGFR* inhibitors and lacks an effective therapy.^{12–22}

Many recent studies have explored the therapeutic strategy for *EGFR* exon 20 insertion mutations, and several candidate inhibitors have been developed.² In a phase II

trial, poziotinib had a confirmed objective response rate of 64% for such mutations.⁴ Another study found that afatinib, an irreversible pan-HER inhibitor, had an 8.7% response rate.²³ Dacomitinib, luminespib, TAK-788, cetuximab with erlotinib and cetuximab with afatinib have been found to have some degree of benefit for patients with tumors harboring such mutations.^{24–28} In addition, tarloxotinib, TAS6417, and compound 1A have also been reported to have inhibitory effects on EGFR exon 20 insertion mutations in preclinical investigations.^{29–31} However, there remains a great need to identify new strategies to overcome the innate drug resistance of NSCLC tumors harboring exon 20 insertions in EGFR.

Erlotinib is a reversible EGFR TKI used to treat non-small cell lung cancer (NSCLC), pancreatic cancer and several other types of cancer. Several researches have shown that erlotinib has a survival benefit in the treatment of lung cancer in phase III trials, and that erlotinib added to chemotherapy improved overall survival by 19%, and improved progression-free survival (PFS) by 29% in unresectable NSCLC, when compared to chemotherapy alone.^{32, 33} In lung cancer, erlotinib has been shown to be effective in patients with *EGFR* mutations containing in-frame deletions of exon 19 and exon 21 L858R point mutation, but appears to be resistant in patients with *EGFR* exon 20 insertion mutations.^{5, 34–36}

Ellagic acid (EA) is a natural phenol compound with antioxidant and antitumor properties that is found in numerous fruits and vegetables, such as pomegranates, cranberries, raspberries, strawberries, grapes and mushrooms. In recent years, the antitumor activity of EA has been extensively investigated in a number of in vitro and in vivo models.^{37–40} Liu *et al.* reported that EA promotes A549 cell apoptosis via regulating the phosphoinositide 3-kinase/protein kinase B pathway.³⁸ Jeong *et al.* claimed that EA inhibits the growth of EGFR TKI-resistant NSCLC cells, HCC827 and H1993.³⁹ Duan *et al.* indicated that EA induces autophagy and exhibits antilung cancer activity in vitro and in vivo.⁴⁰ In this study, the combined antitumor effect of EA with erlotinib was explored in a Ba/F3 cell model harboring *EGFR* H773_V774 insH mutation.

Because there is currently no lung cancer-derived cell line harboring *EGFR* exon 20 insertion mutations, the murine bone marrow-derived cell line, Ba/F3, has generally been used to express such mutations. The advantage of the Ba/F3 model system is the ability to generate cells whose survival depends on mutant *EGFR*.⁴¹ Yasuda *et al.* expressed seven *EGFR* exon 20 insertion mutations in Ba/F3 cells.⁵ Yuza *et al.* obtained three Ba/F3 cell lines expressing *EGFR* exon 20 insertions.³⁶ In this study, we generated a Ba/F3 cell line expressing *EGFR* H773_V774 insH mutation which accounts for approximately 10% of all *EGFR* exon 20 insertion mutations in NSCLC,² and

identified a synergistic strategy by EA with erlotinib against *EGFR* H773_V774 insH mutation. The in vitro results indicated that EA with erlotinib inhibited the growth and clonogenic potential of Ba/F3-insH cells, and promoted cell apoptosis. In a xenograft model of Ba/F3-insH cell line, the combination of EA with erlotinib exhibited synergistic reduction in tumor growth.

Methods

Reagents and compounds

RPMI 1640 medium and fetal bovine serum (FBS) were purchased from Gibco (Invitrogen, Carlsbad, CA, USA). Penicillin-streptomycin (P/S) solution was obtained from Solarbio (Beijing, China). Neo Transfection System and Kits were from Invitrogen (Carlsbad, CA, USA). *EGFR* H773_V774 insH plasmid was purchased from Addgene (Cambridge, MA, USA). The 56 compounds tested for synergy with erlotinib were obtained from BioBioPha Co., Ltd. (Kunming China). Erlotinib was purchased from Selleck Chemicals (Houston, TX, USA). All compounds were dissolved in dimethyl sulfoxide (DMSO; Amresco, Houston, TX, USA) and stored at -20°C until use.

Cell culture

The WEHI cell line (myelomonocytic leukemia, macrophage-like, BALB/c mouse cells; Chinese Academy of Sciences, Kunming, China) was cultured in RPMI 1640 medium supplemented with 10% FBS and 1% P/S. The cell medium was collected every two days and filtered as the source of IL3. The Ba/F3 cell line (Chinese Academy of Sciences, Kunming, China) was maintained in RPMI 1640 supplemented with 10% FBS, 1% P/S, and 1% WEHI-conditioned medium; the medium was changed every two days. All cells were grown at 37°C in a humidified atmosphere with 5% CO_2 .

Ba/F3-insH stable cell line

Ba/F3 cells were cultivated up to approximately 80% confluence on the day of electroporation. Before electroporation, the cells were harvested and washed with phosphate buffered saline (PBS; Solarbio), counted, and resuspended in R resuspension buffer (included with Neon Kits) at a final density of 5×10^7 viable cells/mL. The plates were prepared by filling them with the appropriate volume of culture medium containing FBS and IL3, and preincubated at 37°C in a humidified 5% CO_2 incubator. Then, 0.1 mL sterile plasmid was gently mixed with 0.9 mL cell suspension and electroporation was conducted using the Neon Transfection System at 1600 V, 10 ms, three pulses,

according to the manufacturer's instructions. After electroporation, the cells were immediately transferred to a plate for recovery, and normal medium of Ba/F3 cells was added to the plate 24 hours later. After 48 hours, the medium was changed for IL3-deprived medium containing FBS and P/S. The cells were moved to 96 well plates for the selection of IL3-independent clones. After the selection, cells were subjected to monoclonal. The Ba/F3 cells stably expressed the EGFR-insH mutation were used for subsequent experiments.

Flow cytometry analysis

Expression of the EGFR molecule in transfected Ba/F3 cells was initially assessed by flow cytometry. In brief, IL3-independent cells and untransfected cells (as a negative control) were collected and washed twice in PBS, then stained with fluorescein isothiocyanate (FITC)-conjugated anti-human EGFR antibody (CST, Beverly, MA, USA) for 30 minutes at room temperature, and washed twice with PBS again. Approximately 10 000 events were collected in BD FACS Calibur flow cytometer (BD Bioscience, San Jose, CA, USA) and acquired data were analyzed using FlowJo analysis software version 10 (TreeStar, Inc., Ashland, OR, USA).

Western blotting

Cells for immunoblots were collected and lysed in lysis buffer (Solarbio, Beijing, China) supplemented with protease and phosphatase inhibitors. Samples were placed on ice for 30 minutes and centrifuged at 15 000 rpm for 10 minutes at 4°C. Protein concentrations were determined using a BCA assay (Bio-Rad, San Francisco, CA, USA). Equal amounts of protein (20 µg) were loaded onto SDS-polyacrylamide gels, and transferred to a polyvinylidene difluoride membrane (Millipore, MA, USA). The membranes were blocked in 5% milk and incubated with the indicated primary antibodies, EGFR (1005), PARP, cleaved PARP and Bax from CST (Beverly, MA, USA), TUBB4 from Origin (Rockville, MD, USA). Proteins were detected via incubation with horseradish peroxidase-conjugated secondary antibodies and Pierce ECL Plus western blotting chemiluminescent substrate (4A Biotech Co., Ltd., Beijing, China).

Cell proliferation assays

For IL3-independent assays, 5000 cells/well were plated on 96-well plates, and allowed to grow in RPMI 1640 with or without IL3 for three days. Cell viability was determined using a CellTiter 96 Aqueous One solution proliferation kit (MTS; Promega, Fitchburg, WI, USA) according to the

manufacturer's protocol. For erlotinib sensitivity assays, 10 000 cells/well were inoculated onto 96-well plates, and treated in the appropriate medium with a series concentrations of erlotinib for three days. For the screening of natural compounds,⁴² Ba/F3-insH cells were seeded on 96-well plates in the presence of 1 µM erlotinib with or without 10 µM compounds (each chosen from a library of 56 compounds; see Supporting Information excel) for 72 hours. At the end of this period, cell viability was measured, and compared among samples using a two-tailed Student's *t*-test. A synergy score was developed based on the $-\log_{10}$ of the *P*-value of this *t*-test and was taken to indicate synergistic inhibition of growth (positive score) or antagonism (negative score).

Trypan blue and crystal violet staining assay

Trypan blue staining was used to evaluate cell growth ability of Ba/F3-insH cells. Briefly, cells were plated on 60 mm plates and treated in the appropriate medium with the indicated combination for 48 hours and 72 hours. Cell counts were performed using Trypan blue dye exclusion (Thermo Fisher Scientific, Carlsbad, CA, USA). For crystal violet (Solarbio) staining, Ba/F3-insH cells were seeded on 60 mm plates with agarose medium at a density of 1000 cells per plate, and exposed to the indicated treatment for 11 days, with medium changes once every three days. Cells were fixed with 4% formaldehyde for five minutes, stained with 0.5% crystal violet in the dark for 30 minutes, and washed in flowing water overnight. Photographs of stained cells were obtained using a camera (Canon, Tokyo, Japan).

Cell apoptosis

Cell apoptosis was analyzed by flow cytometry with the following steps. Ba/F3-insH cells were plated on 60 mm plates with the indicated combination for 48 hours or 72 hours. The cells were then obtained and washed twice with cold PBS, and resuspended in 1x binding buffer at a concentration of 1×10^6 cells/mL. Then, 100 µL of the solution (1×10^5 cells) was transferred to a 1.5 mL centrifuge tube, and 5 µL FITC annexin V (BD Bioscience), as well as 5 µL PE propidium iodide (PI; BD Bioscience), were added for cell staining. After incubation for 15 minutes at RT (25°C) in the dark, 400 µL 1x binding buffer was added to each tube, and cell apoptosis was analyzed by flow cytometry within one hour. The following controls were used to set up compensation and quadrants: unstained cells; cells stained with FITC annexin V (no PI); and cells stained with PI (no FITC annexin V).

Animal experiment

Ba/F3-insH cell line xenografts were generated by injecting 5×10^6 cells in 50% matrigel (BD Bioscience) into six- to eight- week old male nu/nu nude mice (Cavens, Changzhou, China). When the tumors had increased to 100 mm^3 , mice were randomized into four treatment groups: 20 mg/kg ellagic acid, 100 mg/kg erlotinib, combination of 20 mg/kg ellagic acid with 100 mg/kg erlotinib

and vehicle control (0.5% Tween-20 in saline). Tumor size was monitored using caliper measurements every two days and the volume was calculated according to the formula (tumor volume = $1/2 \times \text{length} \times \text{width} \times \text{width}$). Bodyweight was measured using an analytical balance every two days, and mice received drugs everyday. Photographs of the tumor and weight were recorded after humanly sacrificing the mice. Experiments were completed in agreement with

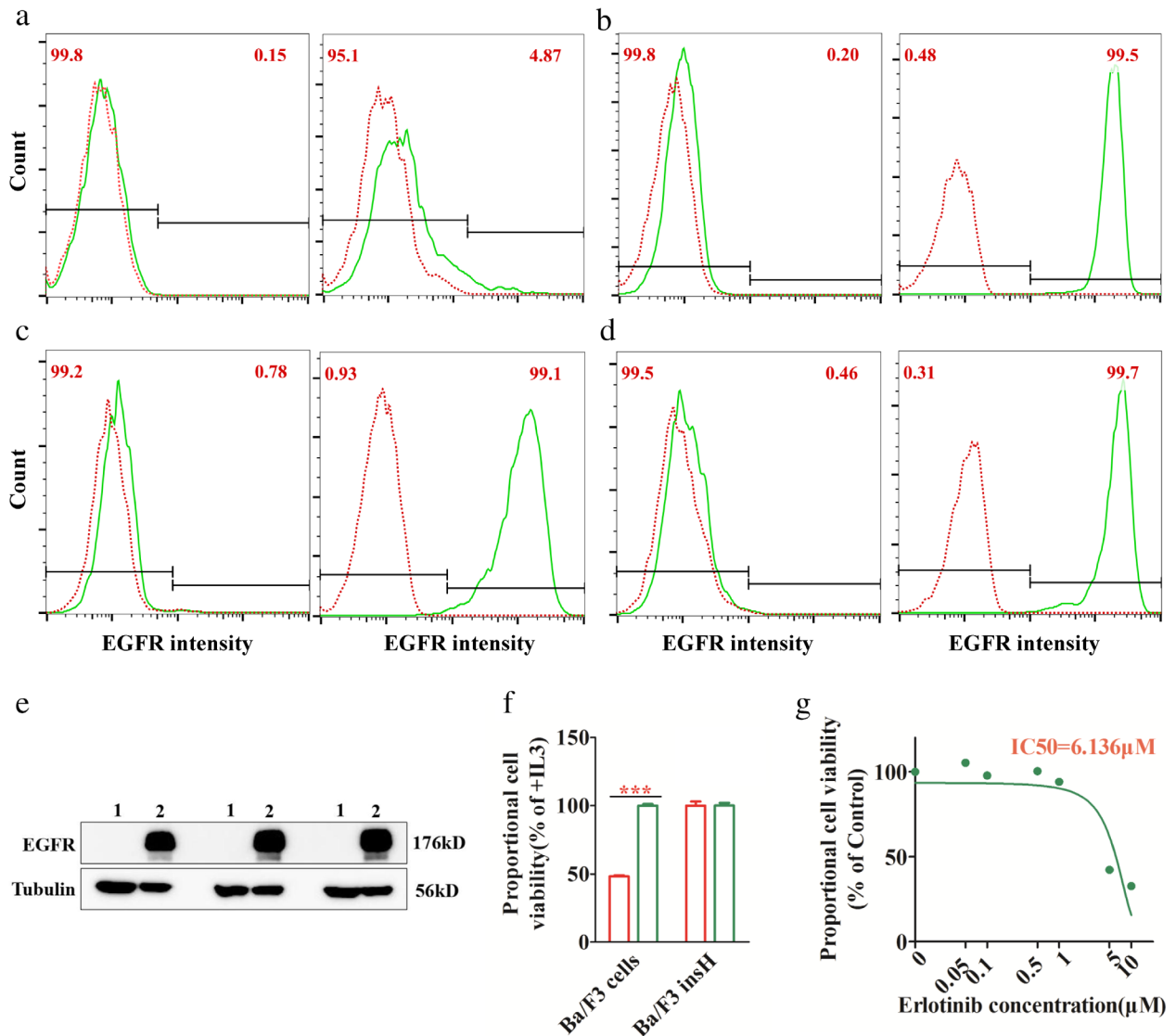


Figure 1 Construction of a stable Ba/F3-insH cell line. (a–d) Flow cytometry results of EGFR expression in transfected cells. (a) Forty-eight hours after electroporation, □P0-C, □P0-S; □P24-C, □P24-S. (b) After selection of IL3-deprivation, □BaF3-C, □BaF3-S, □P-C, □P24-S; (c) After first monoclonal, □BaF3-C, □BaF3-S, □P24-D6G9-C, □P24-D6G9-S; (d) After second monoclonal; left graph, Ba/F3 cells (as a control); right graph, transfected Ba/F3 cells with EGFR-insH plasmid; red dotted line, unstained cells; green solid line, cells stained with specific anti-EGFR antibody, □BaF3-C, □BaF3-S, □P24-D6G9E11-C, □P24-D6G9E11-S. (e) Western blotting results of EGFR and tubulin; 1. Ba/F3 cells, 2. transfected Ba/F3 cells. (f). Transforming ability of EGFR-insH constructs introduced into Ba/F3 cells, IL3-independent growth of Ba/F3 and Ba/F3-insH cells. Values for cells grown without IL3 were normalized to the values for cells grown with IL3; ****P* < 0.0001 (*n* = 6). □-IL3, □+IL3. (g) Response of Ba/F3-insH cells to erlotinib, IC₅₀ value was calculated by GraphPad prism V6 (*n* = 6). The transfection experiments were performed three times.

Good Animal Practices and with approval from Yunnan Agricultural University Animal Care and Use Committee (Kunming, China).

Statistical analysis

The Student's *t*-test was used to determine differences in cell viability between different treatments. $P < 0.05$ was considered statistically significant. We performed our statistical analyses with GraphPad prism version 6 (La Jolla, CA, USA).

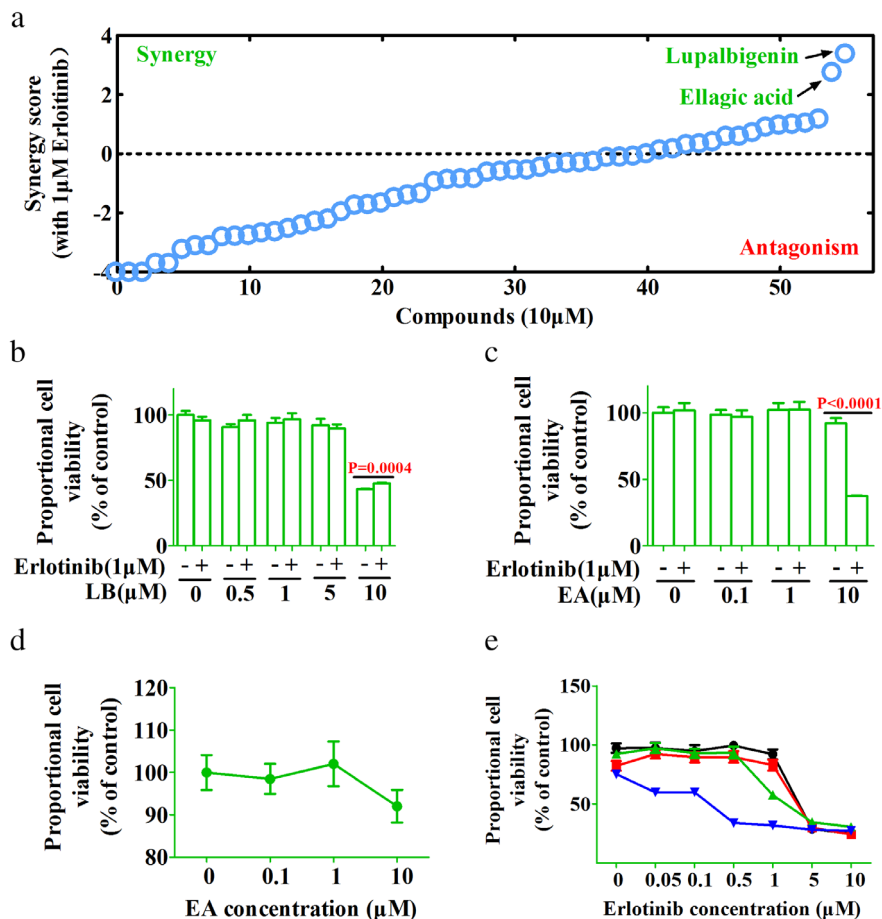
Results

Generation of a stable Ba/F3-insH cell line

The Ba/F3 cell line is able to generate cells whose survival depends on mutant *EGFR*. In this study, to obtain a cell model expressing *EGFR*-insH mutation, we transfected Ba/F3 cells with *EGFR*-insH mutant plasmid by electroporation, and found that approximately 5% transfected cells expressed EGFR on their membrane 48 hours after electroporation (Fig 1a). After a selection with IL3-deprivation,

more than 99% transfected cells harbored EGFR molecules by flow cytometry analysis (Fig 1b). Also, the EGFR expression on transfected Ba/F3 cells was stable after the first and second monoclonal (Fig 1c,d). To further confirm EGFR protein expression, a western blotting assay was performed, and the result showed that EGFR protein was overexpressed in transfected Ba/F3 cells, but not in untransfected Ba/F3 cells (Fig 1e). Having acquired our target cells, we evaluated the transforming ability of *EGFR*-insH mutant as well as the responses of Ba/F3-insH cells to erlotinib using a cell proliferation assay. For the transforming ability of *EGFR*-insH mutant, Ba/F3-insH as well as Ba/F3 cells were subjected to an IL3-independent assay. The viability of Ba/F3-insH cells in the absence of IL3 was near to the presence of IL3, but the proliferation ability of Ba/F3 cells was apparently dependent on IL3 (Fig 1f). These data indicated that the growth of Ba/F3 cells had been transformed in a IL3-independent manner after being transfected with an *EGFR*-insH plasmid. Next, we assessed the response rate of Ba/F3-insH cells to erlotinib. The IC_{50} value was $6.136 \mu\text{M}$ (Fig 1g), almost in agreement with the previous studies.^{5,36}

Figure 2 Synergistic inhibition potential of natural compounds with erlotinib in Ba/F3-insH cells. (a) Result from a combination screen across 56 natural compounds with erlotinib; synergy is based on enhancement of growth inhibition compared to either compound alone. (b) Result of indicated concentrations of lupalbigenin (LB) with erlotinib. (c) Result of indicated concentrations of EA with erlotinib. (d) Dose response curve of EA in Ba/F3-insH cells. (e) Dose-dependent response of Ba/F3-insH cells to erlotinib in the presence of serial concentrations of EA. The concentration-dependent assay of EA with erlotinib was performed three times, ●—DMSO, ■—EA (1 μM), ▲—EA (5 μM), ▼—EA (10 μM).



Combination screen of natural compounds with erlotinib in Ba/F3-insH cells

On the basis of the poor potency of erlotinib toward Ba/F3-insH cells, we sought to identify natural compounds that synergistically inhibit cell viability when combined with erlotinib. Across a library of 56 compounds, both lupalbigenin (LB) and EA exhibited a great synergistic inhibitory effect with erlotinib on the proliferation of Ba/F3-insH cells (Fig 2a). To confirm the efficiency of the two compounds with erlotinib on cell proliferation, we tested a series of concentrations of LB and EA combined with erlotinib and observed that LB had no synergistic effect with erlotinib at all concentrations (Fig 2b), whereas EA showed a synergistic effect with erlotinib at the concentration of 10 μM (Fig 2c), although the effect of EA alone was quite weak (Fig 2d). Next, we detected the response of

Ba/F3-insH cells to erlotinib in the presence of serial concentrations of EA. A dose-dependent assay indicated that the sensitivity of Ba/F3-insH cells to erlotinib was improved in the presence of 5 and 10 μM EA (Fig 2e). These data indicated that EA was able to synergistically inhibit the proliferation of Ba/F3-insH cells with erlotinib.

Effect of ellagic acid with erlotinib on cell growth of Ba/F3-insH cells

To identify the potency of EA with erlotinib toward Ba/F3-insH cells, a trypan blue staining assay was initially recruited to evaluate the effect on cell growth. After treatment with the indicated concentrations of EA with erlotinib for 48 hours, the growth of Ba/F3-insH cells was definitely constrained by 10 μM EA with 1 μM erlotinib

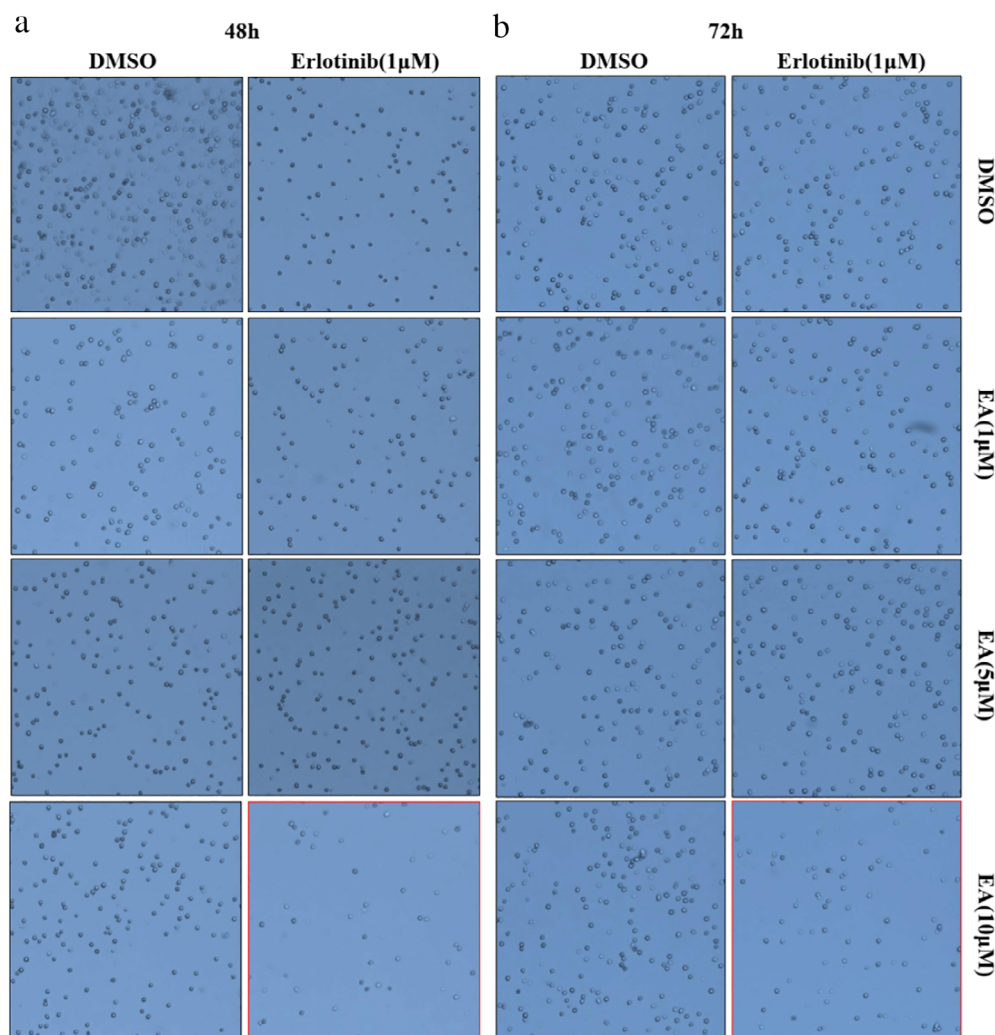


Figure 3 Effect of EA with erlotinib on the growth of Ba/F3-insH cells. (a, b) Graphs of trypan blue staining after treatment with the indicated concentrations of EA with erlotinib for 48 hours (a) and 72 hours (b). The experiment was performed three times.

when compared with control or each compound alone (Fig 3a). A similar result was achieved after treatment for 72 hours (Fig 3b).

Effect of ellagic acid with erlotinib on clonogenic potential of Ba/F3-insH cells

We next assessed the clonogenic potential of Ba/F3-insH cells 11 days after treatment with the indicated compounds. Crystal violet staining was used to display the number of colonies. The photographs indicated that EA partially inhibited the clonogenic potential of Ba/F3-insH cells, erlotinib had virtually no effect, and their combination diminished the clonogenic potential almost completely (Fig 4). The data implied that the combination of EA with erlotinib vastly inhibited the clonogenic potential of Ba/F3-insH cells.

Effect of ellagic acid with erlotinib on cell apoptosis of Ba/F3-insH cells

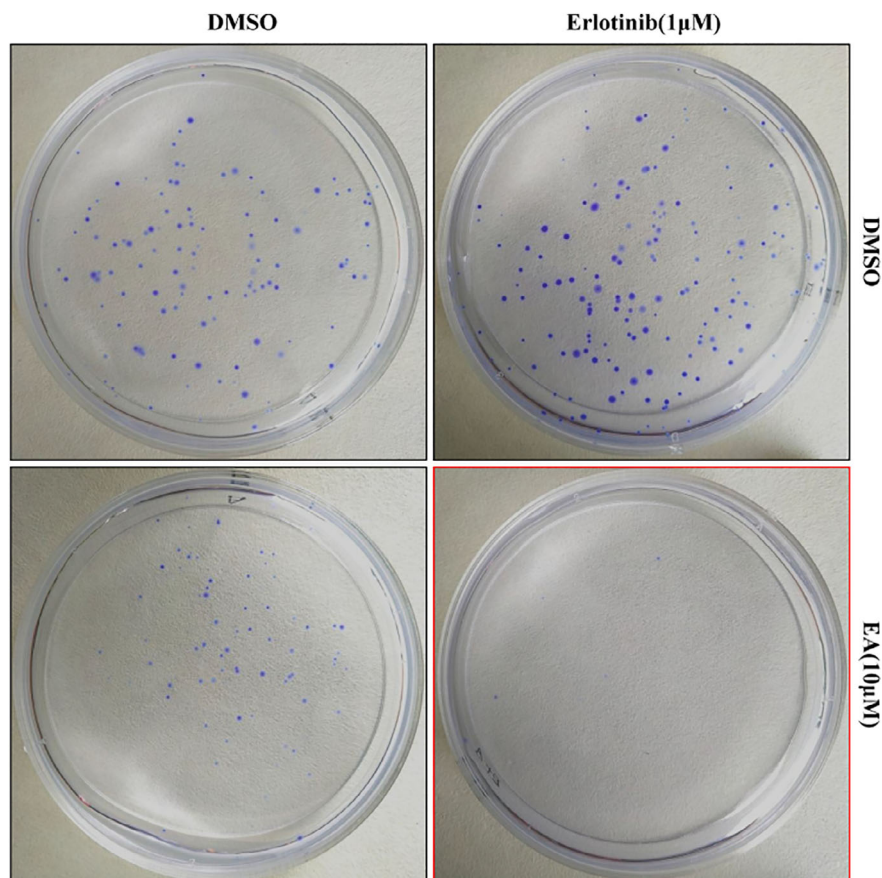
To further evaluate the role of EA with erlotinib in cell apoptosis of Ba/F3-insH cells, we performed a flow

cytometry assay where cells were plated on 60 mm plates and treated with assigned concentrations of EA with erlotinib for 48 hours or 72 hours. The results demonstrated that EA or erlotinib alone had hardly any role in cell apoptosis, and their combination dramatically promoted cell apoptosis 48 hours (Fig 5a) or 72 hours (Fig 5b) after treatment. In addition, the markers of cell apoptosis were detected by western blotting 24 hours after treatment. Result indicated that the expression of cleaved PARP and Bax was vastly increased by combination treatment, when compared to each compound alone (Fig 5c).

Inhibitory effect of ellagic acid with erlotinib on tumor growth of Ba/F3-insH cells in a xenograft model

Given the inhibitory effect of EA with erlotinib in vitro, we tried to explore the potential of EA with erlotinib in a xenograft model of Ba/F3-insH cells. In this study, we created a mice xenograft model with injection of Ba/F3-insH cells. Mice received the indicated treatments after tumor volume reached 100 mm³. Tumor volume and bodyweight were monitored every two days during the period of

Figure 4 Effect of EA with erlotinib on clonogenic potential of Ba/F3-insH cells. Colonies were stained with crystal violet 11 days after treatment with the indicated compounds. The result was representative of two independent experiments.



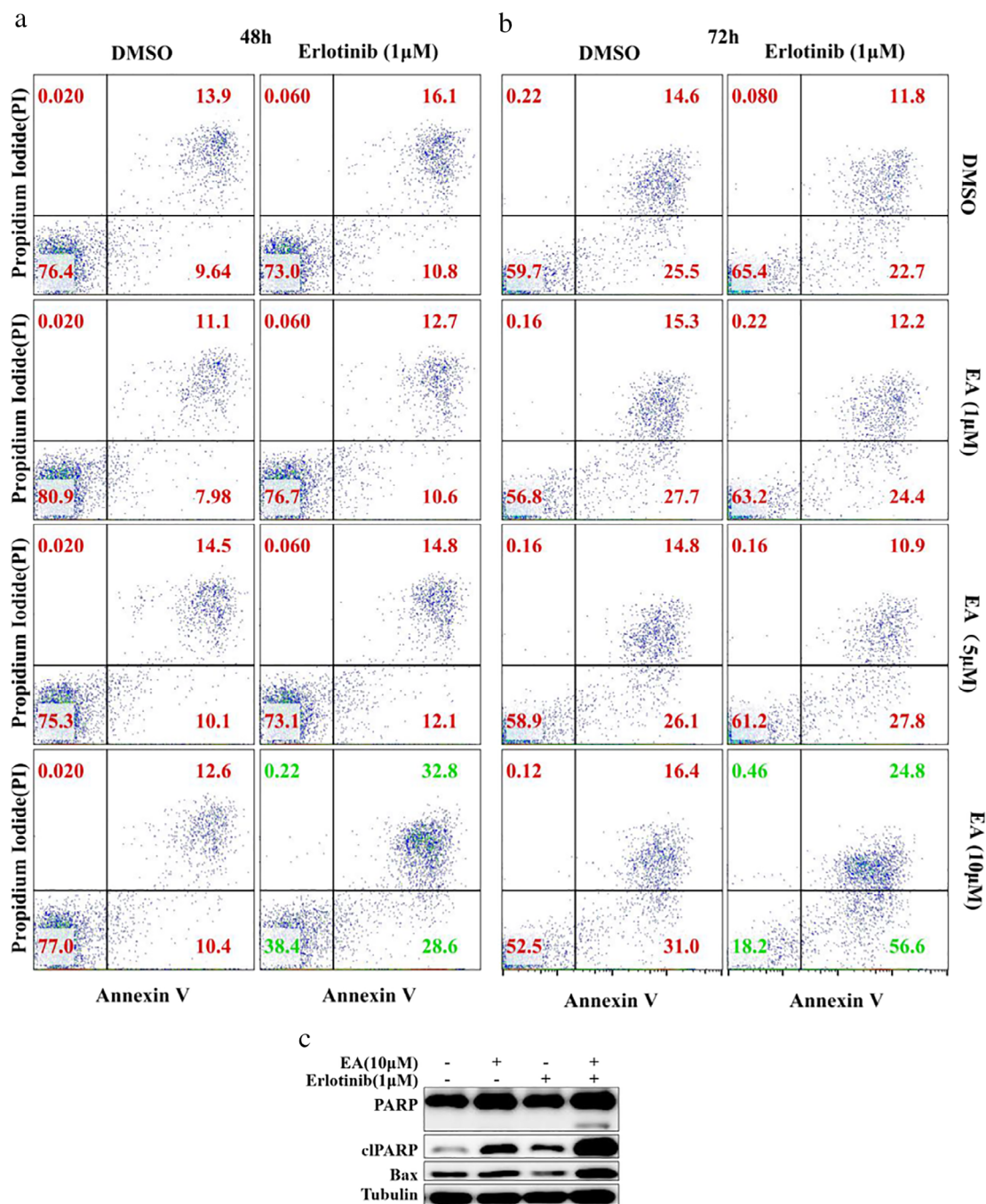
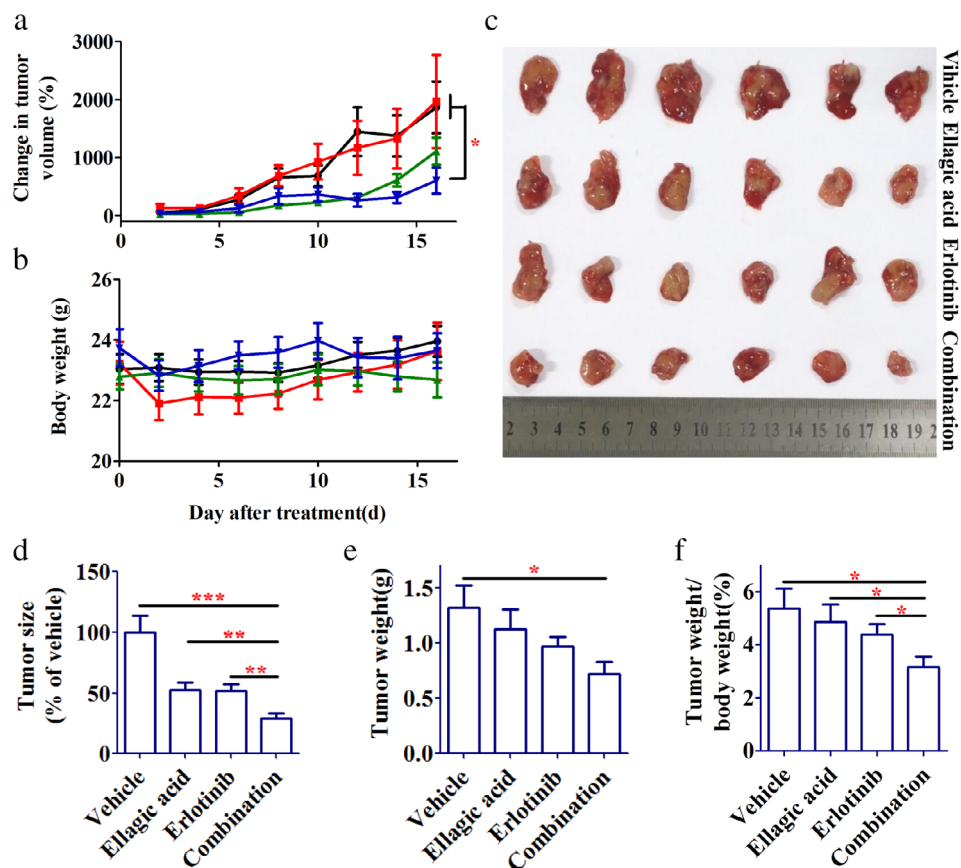


Figure 5 Effect of EA with erlotinib on Ba/F3-insH cell apoptosis. (a, b) Flow cytometry analysis of cells stained with annexin V and propidium iodide (PI) after treatment with the indicated combinations for (a) 48 hours and (b) 72 hours. (c) Western blotting analysis of cells after treatment with the indicated combinations for 24 hours. Result of flow cytometry analysis was representative of three independent experiments, and the western blot analysis was performed twice.

16 days feeding. The data indicated that the change of tumor volume in the combination treatment was obviously decreased in comparison to vehicle and EA alone (Fig 6a), and these treatments had no observed toxicity on the basis

of bodyweight (Fig 6b). After feeding, mice were sacrificed and the tumors were obtained and weighed. The results demonstrated that the tumor size in the combination treatment was smaller than vehicle and each compound alone

Figure 6 Inhibition effect of EA with erlotinib in a xenograft model of Ba/F3-insH cells. (a) Growth of tumors treated with vehicle, 20 mg/kg EA, 100 mg/kg erlotinib or combination for 16 days, *comparison of combination to vehicle or EA alone, ●Vehicle, ■Ellagic acid, ▲Erlotinib, ▼Combination. (b) Change of bodyweight in the period of feeding. (c) Photograph of tumors after mice were sacrificed. (d) A quantitative morphometric analysis of tumor size. (e, f) Tumor weight (e) and value of tumor weight/bodyweight (f) after the mice were sacrificed. Animal experiments were performed once.



(Fig 6c,d), and the tumor weight and the value of tumor weight/bodyweight in the combination treatment were also lower than vehicle (Fig 6e,f).

Discussion

EGFR H773_V774 insH is an insertion mutation within exon 20, and lacks a patient-derived cell line.⁵ In previous studies, several investigators have acquired a number of Ba/F3 cells stably expressing *EGFR* exon 20 insertion mutations.^{5, 36} However, their methods for cell selection were either uneconomical or time-consuming. Hence, we tried to improve the cell selection method when creating a Ba/F3 stable cell line. The results of flow cytometry analysis indicated that more than 99% transfected cells expressed *EGFR* on their membrane after undergoing a process of IL3-deprivation, which proved that the simplified selection method may be available for generation of Ba/F3 stable cell lines expressing *EGFR* mutant.

EGFR exon 20 insertion mutations have been identified as intrinsically resistant to available *EGFR* TKIs and the IC_{50} values of erlotinib were more than micromolar level.^{5, 36} In this study, after acquiring a Ba/F3-insH cell line, we

detected its response to erlotinib, and the IC_{50} value was $6.136 \mu\text{M}$, which is at a same level with the values in previous studies. Next, we explored combination treatment against *EGFR* H773_V774 insH mutation by natural compound with erlotinib. In the screen assay, our data shown that ellagic acid (EA), a plant-derived polyphenol, was the top synergistic candidate for inhibiting cell proliferation. We also determined that $10 \mu\text{M}$ EA with $1 \mu\text{M}$ erlotinib reduced proportional cell viability by more than 50%, while the proportional cell viability was nearly unaffected by EA or erlotinib alone, when compared with the control.

EA is a common metabolite present in many medicinal plants and vegetables with antioxidant, antiatherogenic, anti-inflammatory, and neuroprotective effects.^{43–46} In addition, it is a potential protective agent of the liver and skin and anticancer agent, due to its specific mechanisms that affect cell proliferation, apoptosis, DNA damage, and angiogenesis.⁴⁷ In this study, we identified a combination of EA with erlotinib that strongly inhibited the growth and clonogenic potential of Ba/F3-insH cells, and promoted cell apoptosis, when compared with control or each compound alone. In a xenograft model of Ba/F3-insH cells, the combination treatment significantly reduced the growth of tumor

volume, when compared with vehicle or EA alone, even though there is no significant difference between erlotinib and EA with erlotinib. Taken together, these findings provide a novel strategy for the application of natural compounds. In conclusion, we expressed the *EGFR* H773_V774 insH mutant in a Ba/F3 cell line and identified a combination treatment (EA with erlotinib) against *EGFR* H773_V774 insH mutation.

Acknowledgments

This study was supported by grants from the Major Scientific and Technological Special Project of Yunnan Province (2018IAD60, 2018ZG010 and 2018ZG013). Jun Sheng and Xuanjun Wang conceived and designed the experiments, Chuanqi Xie, Jindong Kong and Fujun Miao performed the experiments, Chuanqi Xie analyzed the data and wrote the paper. All authors have read and agreed to the published version of the manuscript.

Disclosure

The authors declare no conflict of interest.

References

- Bray F, Ferlay J, Soerjomataram I, Siegel RL, Torre LA, Jemal A. Global cancer statistics 2018: GLOBOCAN estimates of incidence and mortality worldwide for 36 cancers in 185 countries. *CA Cancer J Clin* 2018; **68** (6): 394–424.
- Vyse S, Huang PH. Targeting EGFR exon 20 insertion mutations in non-small cell lung cancer. *Signal Transduct Target Ther* 2019; **4**: 5.
- Molina JR, Ping Yang P, Cassivi SD, Schild SE, Adjei AA. Non-small cell lung cancer epidemiology, risk factors, treatment, and survivorship. *Mayo Clin Proc* 2008; **83**: 584–94.
- Robichaux JP, Elamin YY, Tan Z *et al.* Mechanisms and clinical activity of an EGFR and HER2 exon 20-selective kinase inhibitor in non-small cell lung cancer. *Nat Med* 2018; **24** (5): 638–46.
- Yasuda H, Park E, Yun CH *et al.* Structural, biochemical, and clinical characterization of epidermal growth factor receptor (EGFR) exon 20 insertion mutations in lung cancer. *Sci Transl Med* 2013; **5** (216): 1–10.
- Thomas JL, Daphne WB, Raffaella S *et al.* Activating mutations in the epidermal growth factor receptor underlying responsiveness of non-small-cell lung cancer to gefitinib. *N Engl J Med* 2004; **350**: 2129–39.
- Shigematsu H, Lin L, Takahashi T *et al.* Clinical and biological features associated with epidermal growth factor receptor gene mutations in lung cancers. *J Natl Cancer Inst* 2005; **97** (5): 339–46.
- Murray S, Karavasilis V, Bobos M *et al.* Molecular predictors of response to epidermal growth factor receptor antagonists in non-small-cell lung cancer. *J Exp Clin Cancer Res* 2012; **31**: 1–10.
- Riely GJ, Politi KA, Miller VA, Pao W. Update on epidermal growth factor receptor mutations in non-small cell lung cancer. *Clin Cancer Res* 2006; **12** (24): 7232–41.
- Sequist LV, Martins RG, Spigel D *et al.* First-line gefitinib in patients with advanced non-small-cell lung cancer harboring somatic EGFR mutations. *J Clin Oncol* 2008; **26** (15): 2442–9.
- Costa DB, Kobayashi S, Tenen DG, Huberman MS. Pooled analysis of the prospective trials of gefitinib monotherapy for EGFR-mutant non-small cell lung cancers. *Lung Cancer* 2007; **58** (1): 95–103.
- Mitsudomi T, Yatabe Y. Mutations of the epidermal growth factor receptor gene and related genes as determinants of epidermal growth factor receptor tyrosine kinase inhibitors sensitivity in lung cancer. *Cancer Sci* 2007; **98** (12): 1817–24.
- Pao W, Chmielecki J. Rational, biologically based treatment of EGFR-mutant non-small-cell lung cancer. *Nat Rev Cancer* 2010; **10** (11): 760–74.
- Oxnard GR, Lo PC, Nishino M *et al.* Natural history and molecular characteristics of lung cancers harboring EGFR exon 20 insertions. *J Thorac Oncol* 2013; **8** (2): 179–84.
- Arcila ME, Nafa K, Chaft JE *et al.* EGFR exon 20 insertion mutations in lung adenocarcinomas: Prevalence, molecular heterogeneity, and clinicopathologic characteristics. *Mol Cancer Ther* 2013; **12** (2): 220–9.
- Naidoo J, Sima CS, Rodriguez K *et al.* Epidermal growth factor receptor exon 20 insertions in advanced lung adenocarcinomas: Clinical outcomes and response to erlotinib. *Cancer* 2015; **121** (18): 3212–20.
- Jorge SE, Lucena-Araujo AR, Yasuda H *et al.* EGFR exon 20 insertion mutations display sensitivity to Hsp90 inhibition in preclinical models and lung adenocarcinomas. *Clin Cancer Res* 2018; **24** (24): 6548–55.
- Yasuda H, Kobayashi S, Costa DB. EGFR exon 20 insertion mutations in non-small-cell lung cancer: Preclinical data and clinical implications. *Lancet Oncol* 2012; **13** (1): e23–31.
- Riess JW, Gandara DR, Frampton GM *et al.* Diverse EGFR exon 20 insertions and co-occurring molecular alterations identified by comprehensive genomic profiling of NSCLC. *J Thorac Oncol* 2018; **13** (10): 1560–8.
- Yang M, Xu X, Cai J, Ning J, Wery JP, Li QX. NSCLC harboring EGFR exon-20 insertions after the regulatory C-helix of kinase domain responds poorly to known EGFR inhibitors. *Int J Cancer* 2016; **139** (1): 171–6.
- Wu JY, Wu SG, Yang CH *et al.* Lung cancer with epidermal growth factor receptor exon 20 mutations is associated with poor gefitinib treatment response. *Clin Cancer Res* 2008; **14** (15): 4877–82.
- Woo HS, Ahn HK, Lee HY *et al.* Epidermal growth factor receptor (EGFR) exon 20 mutations in non-small-cell lung

- cancer and resistance to EGFR-tyrosine kinase inhibitors. *Invest New Drugs* 2014; **32** (6): 1311–5.
- 23 Yang JCH, Sequist LV, Geater SL *et al.* Clinical activity of afatinib in patients with advanced non-small-cell lung cancer harbouring uncommon EGFR mutations: A combined post-hoc analysis of LUX-lung 2, LUX-lung 3, and LUX-lung 6. *Lancet Oncol* 2015; **16** (7): 830–8.
 - 24 Jänne PA, Ou SHI, Kim DW *et al.* Dacomitinib as first-line treatment in patients with clinically or molecularly selected advanced non-small-cell lung cancer: A multicentre, open-label, phase 2 trial. *Lancet Oncol* 2014; **15** (13): 1433–41.
 - 25 Piotrowska Z, Costa DB, Oxnard GR *et al.* Activity of the Hsp90 inhibitor luminespib among non-small-cell lung cancers harboring EGFR exon 20 insertions. *Ann Oncol* 2018; **29**: 2092–7.
 - 26 Masood A, Kancha RK, Subramanian J. Epidermal growth factor receptor (EGFR) tyrosine kinase inhibitors in non-small cell lung cancer harboring uncommon EGFR mutations: Focus on afatinib. *Semin Oncol* 2019; **46** (3): 271–83.
 - 27 Wheler JJ, Tsimberidou AM, Falchook GS *et al.* Combining erlotinib and cetuximab is associated with activity in patients with non-small cell lung cancer (including squamous cell carcinomas) and wild-type EGFR or resistant mutations. *Mol Cancer Ther* 2013; **12**: 2167–75.
 - 28 van Veggel B, de Langen AJ, Hashemi SMS *et al.* Afatinib and Cetuximab in four patients with EGFR exon 20 insertion-positive advanced NSCLC. *J Thorac Oncol* 2018; **13** (8): 1222–6.
 - 29 Estrada-Bernal A. Abstract A157: Antitumor activity of tarloxotinib, a hypoxia-activated EGFR TKI, in patient-derived lung cancer cell lines harboring EGFR exon 20 insertions. *EGFR/Her2* 2018; **17**: A157.
 - 30 Hasako S, Terasaka M, Abe N *et al.* TAS6417, a novel EGFR inhibitor targeting exon 20 insertion mutations. *Mol Cancer Ther* 2018; **17** (8): 1648–58.
 - 31 Jang J, Son J, Park E *et al.* Discovery of a highly potent and broadly effective epidermal growth factor receptor and HER2 exon 20 insertion mutant inhibitor. *Angew Chem Int Ed* 2018; **57** (36): 11629–33.
 - 32 Cappuzzo F, Ciuleanu T, Stelmakh L *et al.* SATURN: A double-blind, randomized, phase III study of maintenance erlotinib versus placebo following nonprogression with first-line platinum-based chemotherapy in patients with advanced NSCLC. *J Clin Oncol* 2009; **59** (59): 147–7.
 - 33 Gatzemeier U, Pluzanska A, Szczesna A *et al.* Phase III study of erlotinib in combination with cisplatin and gemcitabine in advanced non-small-cell lung cancer: The Tarceva Lung Cancer Investigation Trial. *J Clin Oncol* 2007; **25** (12): 1545–52.
 - 34 Kobayashi K, Hagiwara K. Epidermal growth factor receptor (EGFR) mutation and personalized therapy in advanced nonsmall cell lung cancer (NSCLC). *Target Oncol* 2013; **8** (1): 27–33.
 - 35 Qi WX, Shen Z, Lin F *et al.* Comparison of the efficacy and safety of EGFR tyrosine kinase inhibitor monotherapy with standard second-line chemotherapy in previously treated advanced non-small-cell lung cancer: A systematic review and meta-analysis. *Asian Pac J Cancer Prev* 2012; **13** (10): 5177–82.
 - 36 Yuza Y, Glatt KA, Jiang JR *et al.* Allele-dependent variation in the relative cellular potency of distinct EGFR inhibitors. *Cancer Biol Ther* 2014; **6** (5): 661–7.
 - 37 Ceci C, Lacal PM, Tentori L, De Martino MG, Miano R, Graziani G. Experimental evidence of the antitumor, antimetastatic and antiangiogenic activity of ellagic acid. *Nutrients* 2018; **10** (11): 1756.
 - 38 Liu Q, Liang X, Niu C, Wang X. Ellagic acid promotes A549 cell apoptosis via regulating the phosphoinositide 3-kinase/protein kinase B pathway. *Exp Ther Med* 2018; **16** (1): 347–52.
 - 39 Jeong H, Phan A, Choi JW. Anti-cancer effects of polyphenolic compounds in epidermal growth factor receptor tyrosine kinase inhibitor-resistant non-small cell lung cancer. *Pharmacognosy mag.* 2017; **13** (52): 595–99.
 - 40 Duan J, Zhan JC, Wang GZ, Zhao XC, Huang WD, Zhou GB. The red wine component ellagic acid induces autophagy and exhibits anti-lung cancer activity in vitro and in vivo. *J Cell Mol Med* 2019; **23** (1): 143–54.
 - 41 Jiang J, Greulich H, Janne PA, Sellers WR, Meyerson M, Griffin JD. Epidermal growth factor-independent transformation of Ba/F3 cells with cancer-derived epidermal growth factor receptor mutants induces gefitinib-sensitive cell cycle progression. *Cancer Res* 2005; **65** (19): 8968–74.
 - 42 Shah KN, Bhatt R, Rotow J *et al.* Aurora kinase A drives the evolution of resistance to third-generation EGFR inhibitors in lung cancer. *Nat Med* 2018; **25** (1): 111–8.
 - 43 Vanella L, Giacomo CD, Acquaviva R *et al.* Apoptotic markers in a prostate cancer cell line: effect of ellagic acid. *Oncol Rep* 2013; **30**: 2804–10.
 - 44 Zikri NN, Riedl KM, Wang LS, Lechner J, Schwartz SJ, Stoner GD. Black raspberry components inhibit proliferation, induce apoptosis, and modulate gene expression in rat esophageal epithelial cells. *Nutr Cancer* 2009; **61** (6): 816–26.
 - 45 Ceci C, Tentori L, Atzori MG *et al.* Ellagic acid inhibits bladder cancer invasiveness and in vivo tumor growth. *Nutrients* 2016; **8**: 1–20.
 - 46 Stoner GD. Foodstuffs for preventing cancer: The preclinical and clinical development of berries. *Cancer Prev Res* 2009; **2** (3): 187–94.
 - 47 Ríos JL, Giner R, Marín M, Recio M. A pharmacological update of ellagic acid. *Planta Med* 2018; **84** (15): 1068–93.